crystals

MDPI

Article

Progress in Near-Equilibrium Ammonothermal (NEAT) Growth of GaN Substrates for GaN-on-GaN Semiconductor Devices

Tadao Hashimoto *, Edward R. Letts and Daryl Key

SixPoint Materials, Inc., Buellton, CA 93427, USA; ed@spmaterials.com (E.R.L.); daryl@spmaterials.com (D.K.)
* Correspondence: tadao@spmaterials.com

Abstract: This paper reviews the near-equilibrium ammonothermal (NEAT) growth of bulk gallium nitride (GaN) crystals and reports the evaluation of 2″ GaN substrates and 100 mmbulk GaN crystal grown in our pilot production reactor. Recent progress in oxygen reduction enabled growing NEAT GaN substrates with lower residual oxygen, coloration, and optical absorption. The oxygen concentration was approximately 2×10^{18} cm^{-2}, and the optical absorption coefficient was 1.3 cm^{-1} at 450 nm. Maps of full-width half maximum (FWHM) of X-ray diffraction rocking curveswere generated for grown crystals and finished wafers. The X-ray rocking curve maps confirmed high-quality and uniform microstructure across the entire surface of the bulk crystals and substrates. The average FWHM of the 50 best bulk crystals from the recent batch was 28 ± 4 arcsec for the 002 diffraction and 34 ± 5 arcsec for the 201 diffraction, with an average radius of curvature of 20 m. X-ray topography measured on both sides of the bulk crystals implied that the density of dislocations wasreduced by one order of magnitude during the NEAT growth. A typical NEAT GaN substrate shows dislocation density of about 2×10^{5} cm^{-2}.

Keywords: bulk GaN; ammonothermal growth; GaN substrate; NEAT method

Citation: Hashimoto, T.; Letts, E.R.; Key, D. Progress in Near-Equilibrium Ammonothermal (NEAT) Growth of GaN Substrates for GaN-on-GaN Semiconductor Devices. *Crystals* **2022**, *12*, 1085. https://doi.org/10.3390/cryst12081085

Academic Editor: Younes Hanifehpour

Received: 11 July 2022
Accepted: 30 July 2022
Published: 3 August 2022

1. Introduction

Gallium nitride (GaN) is one of the wide bandgap semiconductors. Successful commercialization of GaN-based light-emitting diodes (LEDs) has promoted further research and development of GaN for other applications, including laser diodes (LDs), high electron mobility transistors (HEMTs), and power transistors. However, except for LDs, the majority of GaN devices are developed using dissimilar substrates, such as sapphire, silicon carbide (SiC), and silicon (Si). Usage of low-cost substrates, such as sapphire and silicon, is mandatory for applications in consumer electronics, where cost-reduction pressure is extremely high. Nevertheless, new applications are currently emerging in the energy, defense, and industrial sectors. Devices in these sectors require reliable high-power operation, which is often more important than cost. Since heteroepitaxial growth generates threading dislocations that degrade device performance and lifetime [1], homoepitaxial GaN substrates with lower dislocation density are of interest despite their higher price.

Although hydride vapor phase epitaxy (HVPE) is currently used to produce the majority of GaN substrates in the marketplace, the method shows limitations in achieving low dislocation density. Several non-vapor phase methods including high-pressure solution growth [2–4], flux growth [5–10], and ammonothermal growth [11–22] have been researched. We have developed the near-equilibrium ammonothermal (NEAT) method to produce low-dislocation GaN substrates. The NEAT method is one type of ammonothermal growth with growth conditions set near equilibrium. Utilizing a weak driving force enables continuous growth for months through a reduction in spontaneous nucleation. The NEAT condition achieves improvement in crystal quality over the growth period. The drawback of a lower growth rate is offset by an increase in the number of bulk GaN crystals grown per batch.

In 2018, we successfully demonstrated 2″ crack-free GaN substrates [23]. However, GaN crystals grown by the ammonothermal method typically contained high levels of oxygen in the order of 10^{19} cm^{-3}. Previously reported 2″ substrates also contained 10^{19} cm^{-3} of oxygen and the color was light brown [23]. In 2019, we successfully reduced the oxygen concentration in small-sized NEAT bulk GaN [24]. Scaling up the same oxygen reduction strategy to a large production reactor, we successfully grew reduced-color 2″ bulk GaN crystals. This paper reports the characterization of reduced-oxygen 2″ NEAT GaN substrates. In addition, by using the same pilot-production reactor, we attempted growth of 4″ bulk GaN. We confirmed that the dislocation density in the 4″ bulk GaN was similar to our 2″ bulk GaN.

2. Experiment

GaN bulk crystals were grown by the NEAT method using our pilot-production high-pressure reactor. Single crystalline GaN seed crystals, polycrystalline GaN and/or metallic Ga, and an alkali-based mineralizer were loaded into the reactor. After sealing the reactor, the air inside the reactor was pumped out and replaced with anhydrous ammonia. The ammonia fill factor was 40~60%. Then, the reactor was heated with external heaters to 450–600 °C. The resulting ammonia pressure was 100~300 MPa. The driving force of crystal growth was controlled with growth parameters including temperature, pressure, seed location, and nutrient location. In the NEAT method, we controlled the driving force to achieve consistent growth over a few months.

Seed crystals were prepared by HVPE. As reported previously, the microstructure of seed crystals has a significant impact on the quality of grown bulk crystals [25]. Low-quality seed crystals were filtered out from usage by evaluating a mapping of X-ray full-width half maximums (FWHMs) over the wafer, as outlined below. Selected seeds typically showed an average FWHM of 002 rocking curves less than 100 arcsec with a radius of curvature of about 5–10 m. The lateral sizes of the seed crystals were 2″, 2.3″, or 4″.

After the NEAT growth, photographs of grown crystals were taken with a digital camera (Canon, Powershot SX510RX). The bulk crystals were rounded with a core drill and a cylindrical grinder. After making a primary orientation flat on the m-plane and a secondary orientation flat on the a-plane, the bulk GaN crystals were sliced into wafers with a multiple wire saw. Sliced GaN blank wafers were shaped with a surface grinder, polished, and finished with chemical mechanical polishing (CMP). Additional details regarding the wafering process are outlined in a previous paper [26]. Removal of the subsurface damaged layer after CMP was confirmed by measuring the intensity of the shoulders of the 114 rocking curve in a grazing configuration [27]. The incident beam angle was 10.8662° to the Ga surface of the wafer. The intensity of shoulders was compared with an empirically obtained standard peak from an unprocessed bulk GaN crystal with no processing-related surface or subsurface damage. Surface morphology of samples was observed with a Nomarski microscope and a tapping-mode atomic force microscope (AFM, Asylum MFP-3D).

After the double-side CMP, optical absorption of the GaN substrates was measured using a spectrophotometer (Shimazu UV-2401PC). Secondary ion mass spectroscopy (SIMS) was measured at EAG Inc. The depth profile of oxygen was measured for smaller-sized GaN crystals co-loaded in the production growth. The oxygen detection limit was about 8×10^{15} cm^{-3}.

The qualities of seed crystals, grown bulk crystals, and processed wafers were characterized with an X-ray diffractometer (PANalytical X'Pert) using a Cu Kα X-ray source and a four-crystal Ge (002) monochromator. The X-ray source was operated at 40 mA and 40 kV. Seeds, grown crystals, and processed wafers were routinely characterized by mapping the FWHMs of X-ray rocking curves from the 002 and 201 diffractions over the entire wafer. The spatial separation of each measuring point was 2 mm. To obtain sufficient spatial separation of the incident X-ray beam, 0.3 mm × 0.3 mm slits were used after the

monochromator. The estimated X-ray beam sizes on the sample were 0.3 mm × 1.0 mm and 1.17 mm × 0.52 mm for the 002 and 201 measurements, respectively.

The X-ray topography was measured at the BL16B2 of SPring-8 synchrotron radiation facility in Japan. The X-ray beam was monochromated with a Si (111) double crystal monochromator. The X-ray beam with 9.16 keV of energy was irradiated onto the sample with an incident angle of about 3°, and the topography image from the (114) reflection at $2\theta = 84.6°$ was recorded on an X-ray film.

3. Results and Discussion

3.1. Appearance, Coloration, and Optical Absorption

After the growth, photographs of the crystals were taken with a digital camera. Figure 1 shows bulk GaN crystals grown in one batch. As demonstrated here, we can grow many crystals simultaneously by using a large-sized pressure reactor. Simultaneous growth of many crystals offsets the low growth rate (approximately 30 μm per day). This is the advantage of the ammonothermal method over the other growth methods.

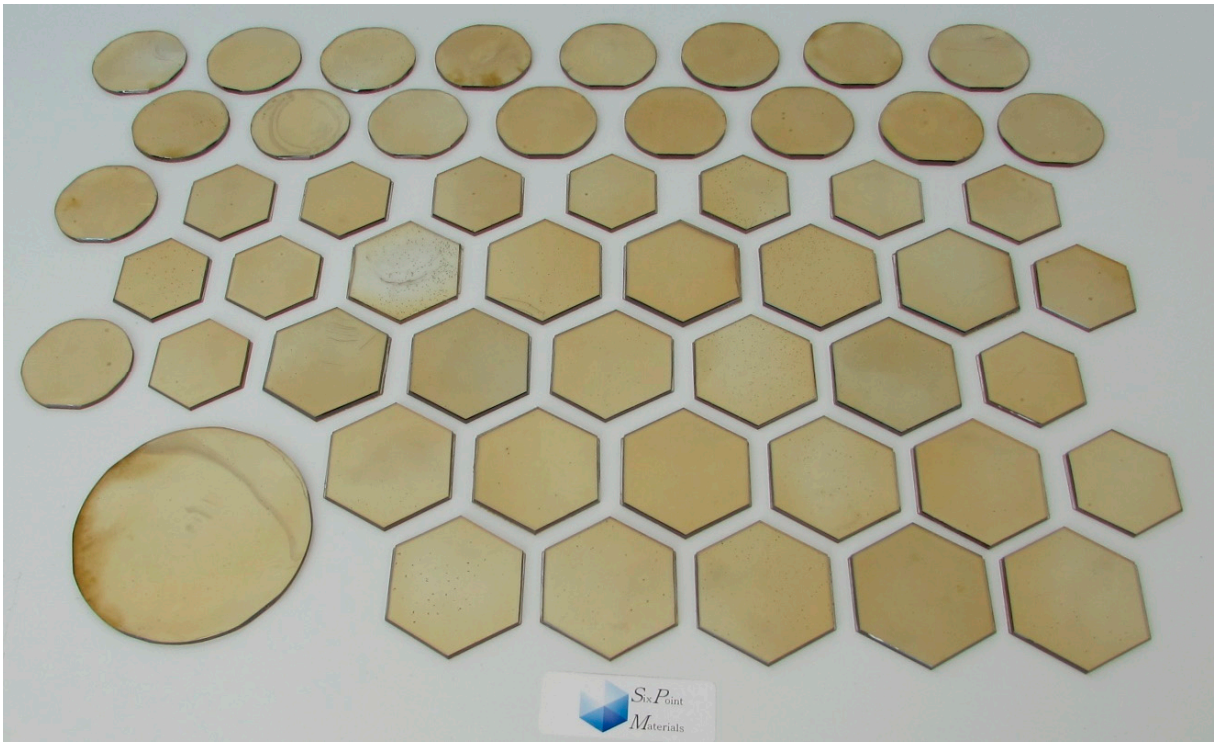

Figure 1. A photograph of bulk GaN crystals grown in one batch. The largest round crystal is approximately 100 mm in diameter and the other round crystals have approximately 50 mm in diameter. The larger hexagonal crystals have a side-to-side width of approximately 50 mm and the smaller hexagonal crystals have a point-to-point width of approximately 50 mm.

Figure 2 shows a comparison of two crystals from different runs, before (left) and after (right) implementation of our improved oxygen removal procedure in the pilot production reactor. The picture shows that the crystal coloration was greatly reduced with better oxygen removal in the growth environment. The residual oxygen in co-loaded smaller crystals was 7.5×10^{18} cm^{-3} for the previous run and 1.5×10^{18} cm^{-3} for the latest run.

A photograph of a 2″ GaN substrate after single-side CMP is presented in Figure 3. The substrate looks almost colorless relative to the crystal it was sliced from, because the thickness of the substrate is much thinner, about 400 μm. We confirmed removal of the subsurface damaged layer in the finished wafer with grazing angle X-ray diffraction [27]. AFM images were not recorded for all substrates, because it potentially damages the

finished surface. However, the surface typically shows an atomic step structure after CMP, as reported previously [23].

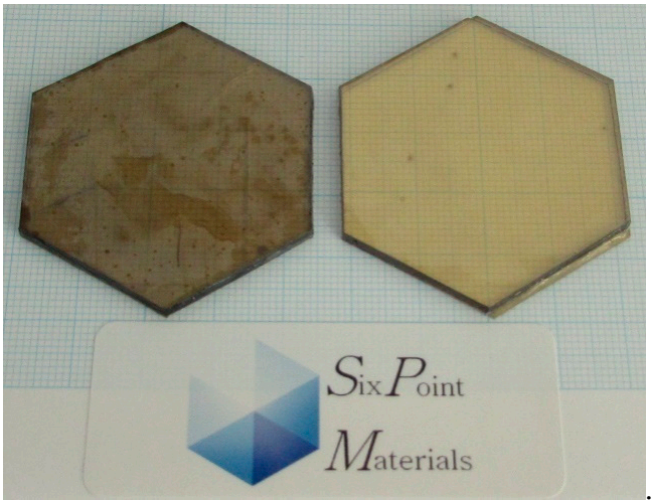

Figure 2. A photograph of bulk GaN crystals grown in the previous higher-oxygen condition (**left**) and the latest lower-oxygen condition (**right**). Coloration was significantly reduced.

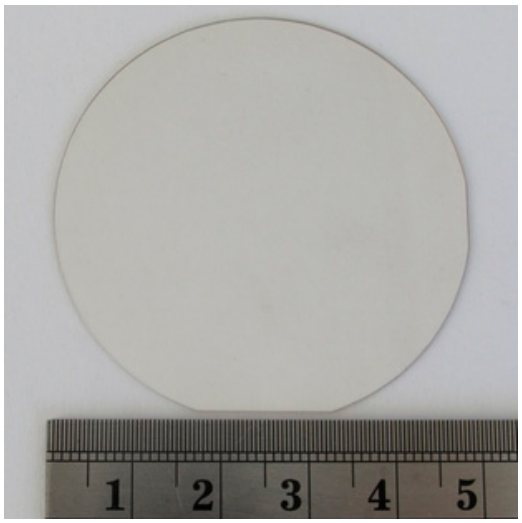

Figure 3. A photograph of 2″ diameter lower-oxygen NEAT GaN substrate after single-side polishing.

Optical absorption was measured for double-side polished substrates. The absorption coefficient of GaN substrates in the previous high-oxygen growth was 5.6 cm^{-1} at 450 nm, whereas that from the reduced-oxygen growth was 1.3 cm^{-1} at 450 nm. These results are in line with our previous results. Figure 4 shows the relationship between the optical absorption coefficient at 450 nm and the residual oxygen concentration in the NEAT substrates. As shown in the figure, the optical absorption shows direct correlation with the residual oxygen concentrations for the oxygen concentration from 1.5×10^{18} cm^{-3} to 2.5×10^{20} cm^{-3}.

3.2. X-ray Mapping

X-ray FWHM maps were measured for 2″ NEAT GaN substrates after CMP. Figure 5a shows an example of a FWHM map for 002 rocking curves, and Figure 5b shows a map for 201 rocking curves. For this particular sample, average FWHMs were 28 arcsec for the 002 diffraction and 36 arcsec for the 201 diffraction. The higher 201 FWHM was due to higher values in the right-edge region of the substrate. The average FWHM of the 50 best bulk crystals from the batch shown in Figure 1 was 28 ± 4 arcsec for the 002 diffraction

and 34 ± 5 arcsec for the 201 diffraction, with an average radius of curvature of 20 m. This indicates the crystals are of excellent quality. We expect additional wafers from these bulk crystals to have similar X-ray FWHM numbers to the bulk crystals they are sliced from.

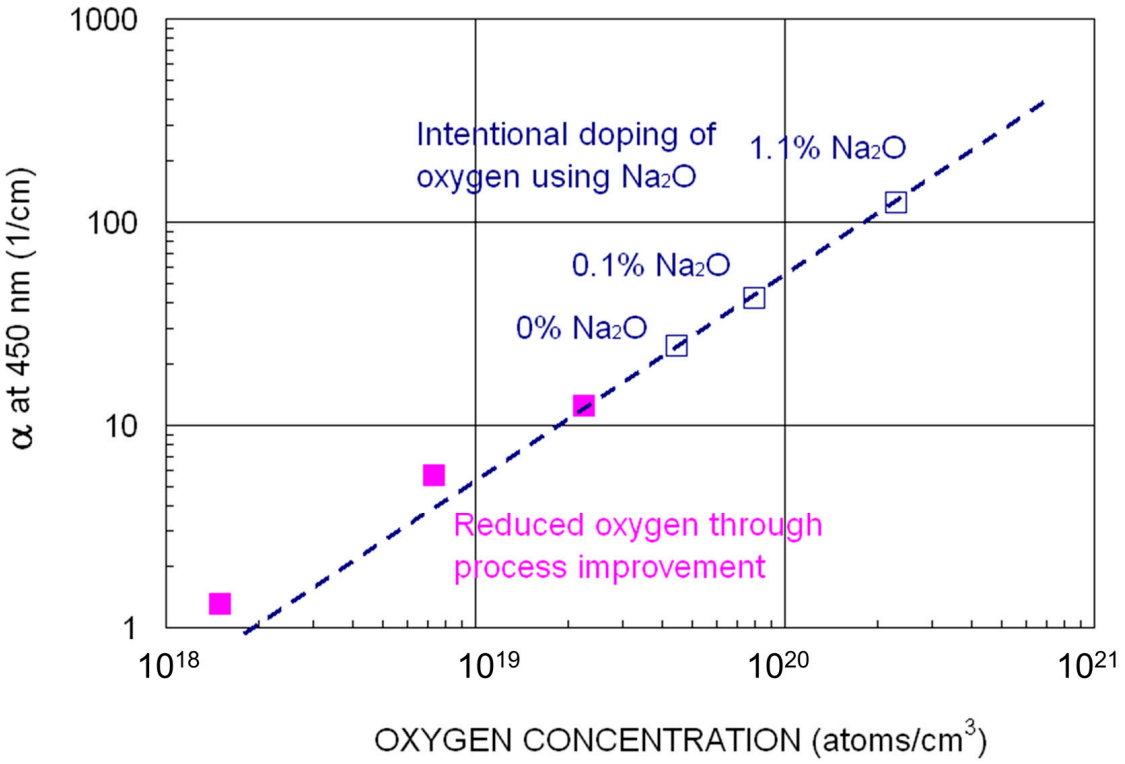

Figure 4. Relationship between the optical absorption coefficient at 450 nm and the residual oxygen concentration in the crystal.

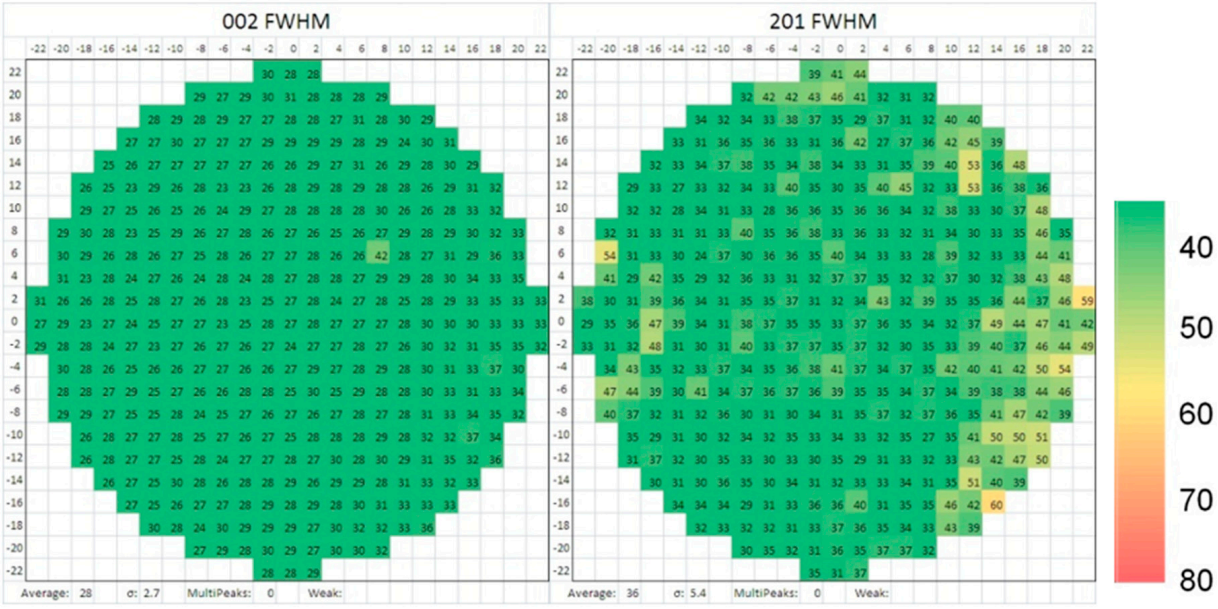

Figure 5. X-ray FWHM maps of a 2″ NEAT GaN substrate. The numbers on each axis present position from the center in mm, and the numbers in the boxes and next to the scale bar are the FWHM values in arcsec. (**a**) FWHM of 002 rocking curves; (**b**) FWHM of 201 rocking curves.

The X-ray maps for HVPE-grown substrates highlight the superior microstructure uniformity of NEAT GaN substrates. Figure 6a shows an sample X-ray FWHM map for 002 rocking curves, and Figure 6b shows a map for 201 rocking curves. The HVPE substrate shows more yellow and even red regions for both the 002 and 201 maps. Additionally, some spots show double peaks and triple peaks in rocking curves, represented by a single diagonal line and double diagonal lines in the box, respectively.

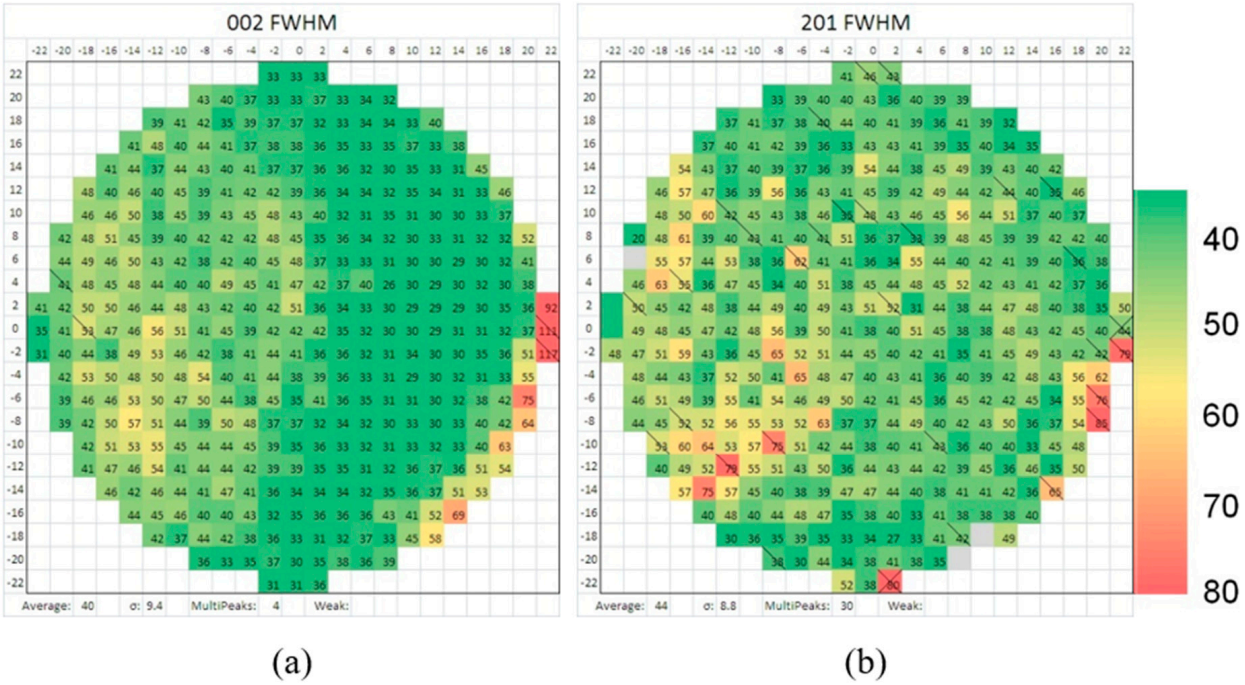

Figure 6. X-ray FWHM maps of a 2″ GaN substrate produced by HVPE. The numbers on each axis present position from the center in mm, and the numbers in the boxes and next to the scale bar are the FWHM value in arcsec. Boxes with a single diagonal line indicate a double peak in the rocking curve and boxes with double diagonal lines indicate a triple peak in the rocking curve. (**a**) FWHM of 002 rocking curves; (**b**) FWHM of 201 rocking curves.

From these results, it is clear that measuring X-ray FWHM at one or several points can yield a misleading evaluation of the GaN substrates. There are many green spots in the HVPE GaN substrates. If the selected measurement spot falls into such green zones, one will obtain narrow X-ray rocking curves and may expect that the substrate has high quality everywhere. The X-ray FWHM mapping we employ is a powerful tool to evaluate crystal quality and uniformity of GaN substrates. These X-ray FWHM maps demonstrate the superior microstructure of 2″ NEAT GaN substrates.

3.3. Growth and Characterization of 4″ Bulk GaN Crystal

A photo of the 100 mm diameter bulk GaN crystal after rounding and flat formation is presented in Figure 7. The dark stain around the edge is a roughened surface caused by precipitation of the alkali mineralizer during cool-down at the end of the growth. We surmise that the concentrated alkali metal-based compound etched the surface of the crystal. The oxygen concentration was 1.32×10^{18} cm^{-3} on the top surface of the crystal, i.e., the final oxygen concentration at the end of the growth. The dots did not extend through the thickness of the growth. They were holes in the HVPE seed that closed early in the NEAT growth. The ability of the NEAT growth to close holes is a clear advantage over HVPE, where holes grow larger with time, limiting the run time and growth thickness [28]. Holes in the substrate cause problems during device fabrication, and substrates with holes are sold at a lower price tier.

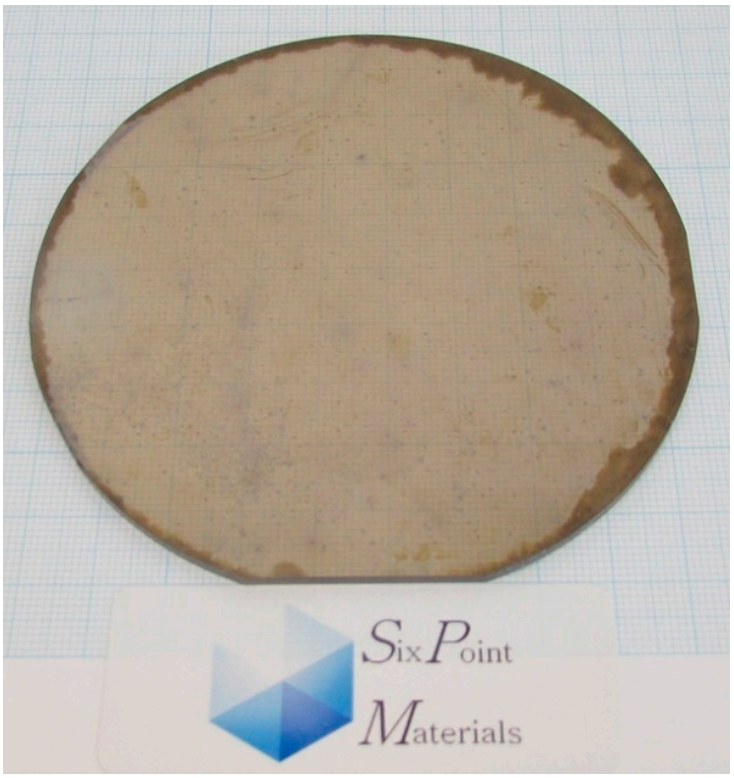

Figure 7. A photograph of 100 mm-diameter bulk GaN crystals grown by the NEAT method.

X-ray topography was measured on both sides of the boule (Figure 8). Since the Ga polar surface of the seed crystal was masked during the growth, *c*-plane growth only occurred on the N-polar face. Therefore, the Ga-polar side of the boule exposed the seed. Figure 8a shows an X-ray topography image of the as-grown N-polar face of the boule. Due to the lattice bow of the sample, the image area with constructive reflection is sandwiched between off-Bragg regions covered with many white islands (top and bottom regions in the image). The white dots in the dark region of the image (one example is indicated with a white arrow), are contrasts of threading dislocations. Although detailed analysis is needed, we think that the majority of the dislocations are either edge or mixed dislocations. The dislocation density counted from the two areas indicated with white 200 × 200 μm squares was about 2×10^5 cm^{-2} and 5×10^5 cm^{-2}.

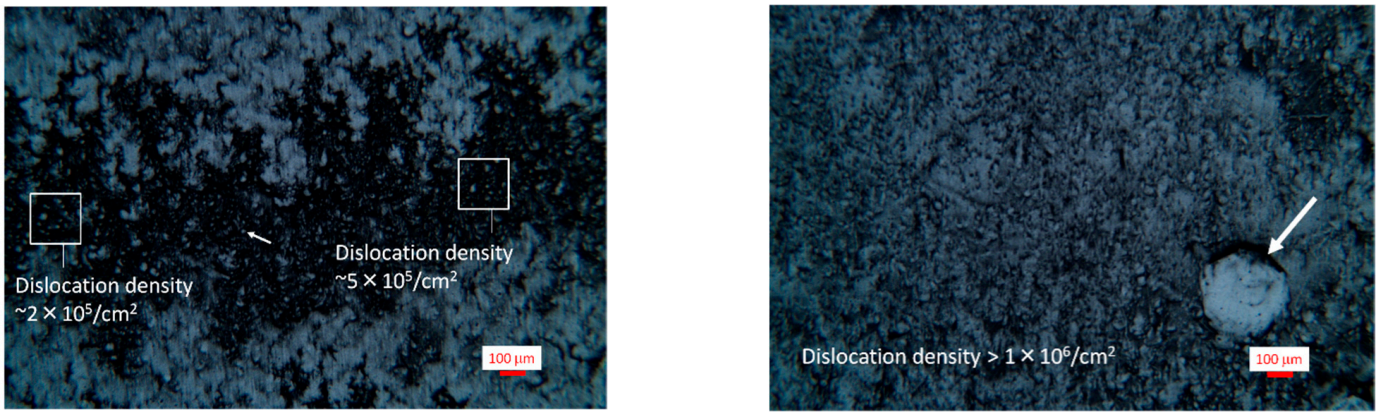

(**a**) (**b**)

Figure 8. X-ray topography from the 100 mm-bulk GaN crystal. (**a**) From as-grown N-polar surface; (**b**) from Ga-polar surface which exposes Ga-face of the HVPE seed.

Figure 8b shows an X-ray topography image from the Ga-polar surface of the boule, which was the seed crystal. As shown in the image, the defect density was so high that it was practically impossible to adequately distinguish one dislocation contrast from another; hence, the estimated dislocation density was greater than 10^6 cm^{-2}. In addition, the seed image shows a macro defect, as indicated with a white arrow. It was confirmed that the dislocation density was improved from >10^6 cm^{-2} level to 2~5 × 10^5 cm^{-2} during the NEAT growth of 100 mm bulk GaN.

4. Conclusions

Bulk GaN crystals of 2″ and 4″ were grown by the NEAT method. The 2″ GaN substrates produced by the NEAT method were characterized with optical observation methods, X-ray rocking curves, and X-ray topography. The latest NEAT GaN substrate had a reduced oxygen concentration of 1.5 × 10^{18} cm^{-3}. The optical absorption coefficient at 450 nm was 1.3 cm^{-1}, which followed the trend line of the previously reported relationship between the absorption coefficient and oxygen concentration. FWHM mapping of X-ray rocking curves and X-ray topography both demonstrated high degrees of crystalline perfection in the 2″ substrates. The dislocation density was estimated to be low-10^5 cm^{-2} from the X-ray topography. A 100 mm bulk GaN crystal grown by the NEAT method also showed reduced dislocation density (2~5 × 10^5 cm^{-2}) from that of the seed crystal.

Author Contributions: Data curation, E.R.L. and D.K.; Funding acquisition, T.H.; Project administration, T.H.; Writing—original draft, T.H.; Writing—review & editing, E.R.L. and D.K. All authors have read and agreed to the published version of the manuscript.

Funding: This research was funded by Advanced Research Projects Agency-Energy (Grant No. DE-AR0000445 and DE-AR0001008), US Department of Energy (Grant No. DE-SC0013791 and DE-LC000L059), The Office of Naval Research (Grant No. N00014-19-1-2069).

Acknowledgments: The synchrotron radiation experiments were performed at the BL16B2 of Spring-8 with the approval of Japan Synchrotron Radiation Research Institute (JASRI) (Proposal No. 2021B5370). The authors thank Masakazu Kanechika at Nagoya University and Satoshi Yamaguchi, Kosuke Kitazumi, and Yasuji Kimoto at Toyota Central R&D Labs., Inc. for the X-ray topography measurement.

Conflicts of Interest: The authors declare no conflict of interest.

References

1. Nakamura, S. InGaN-based blue light-emitting diodes and laser diodes. *J. Cryst. Growth* **1999**, *201–202*, 290–295. [CrossRef]
2. Porowski, S. Bulk and homoepitaxial GaN-growth and characterisation. *J. Cryst. Growth* **1998**, *189–190*, 153–158. [CrossRef]
3. Inoue, T.; Seki, Y.; Oda, O.; Kurai, S.; Yamada, Y.; Taguchi, T. Growth of bulk GaN single crystals by the pressure-controlled solution growth method. *J. Cryst. Growth* **2001**, *229*, 35–40. [CrossRef]
4. Bockowski, M.; Strak, P.; Grzegory, I.; Lucznik, B.; Porowski, S. GaN crystallization by the high-pressure solution growth method on HVPE bulk seed. *J. Cryst. Growth* **2008**, *310*, 3924–3933. [CrossRef]
5. Yamane, H.; Shimada, M.; Sekiguchi, T.; DiSalvo, F.J. Morphology and characterization of GaN single crystals grown in a Na flux. *J. Cryst. Growth* **1998**, *186*, 8–12. [CrossRef]
6. Aoki, M.; Yamane, H.; Shimada, M.; Sarayama, S.; DiSalvo, F.J. Conditions for seeded growth of GaN crystals by the Na flux method. *J. Cryst. Growth* **2002**, *56*, 660–664. [CrossRef]
7. Wang, W.J.; Chen, X.L.; Song, Y.T.; Yuan, W.X.; Cao, Y.G.; Wu, X. Assessment of Li-Ga-N ternary system and GaN single crystal growth. *J. Cryst. Growth* **2004**, *264*, 13–16. [CrossRef]
8. Kawamura, F.; Morishita, M.; Tanpo, M.; Imade, M.; Yoshimura, M.; Kitaoka, Y.; Mori, Y.; Sasaki, T. Effect of carbon additive on increases in the growth rate of 2 in GaN single crystals in the Na flux method. *J. Cryst. Growth* **2008**, *310*, 3946–3949. [CrossRef]
9. Konishi, Y.; Masumoto, K.; Murakami, K.; Imabayashi, H.; Takazawa, H.; Todoroki, Y.; Matsuo, D.; Maruyama, M.; Imade, M.; Yoshimura, M.; et al. Growth of Prismatic GaN Single Crystals with High Transparency on Small GaN Seed Crystals by Ca-Li-Added Na Flux Method. *Appl. Phys. Express* **2012**, *5*, 025503. [CrossRef]
10. Hayashi, M.; Imanishi, M.; Yamada, T.; Matsuo, D.; Murakami, K.; Maruyama, M.; Imade, M.; Yoshimura, M.; Mori, Y. Enhancement of lateral growth of the GaN crystal with extremely low dislocation density during the Na-flux growth on a point seed. *J. Cryst. Growth* **2017**, *468*, 827–830. [CrossRef]
11. Peters, D. Ammonothermal synthesis of aluminum nitride. *J. Cryst. Growth* **1990**, *104*, 411–418. [CrossRef]

12. Dwilinski, R.; Baranowski, J.M.; Kaminska, M. On GaN crystallization by ammonothermal method. *Acta Phys. Pol. A* **1996**, *90*, 763–766. [CrossRef]
13. Ketchum, D.R.; Kolis, J.W. Crystal growth of gallium nitride in supercritical ammonia. *J. Cryst. Growth* **2001**, *222*, 431–434. [CrossRef]
14. Purdy, A.P.; Jouet, R.J.; George, C.F. Ammonothermal Recrystallization of Gallium Nitride with Acidic Mineralizers. *Cryst. Growth Des.* **2002**, *2*, 141–145.
15. Hashimoto, T.; Fujito, K.; Wu, F.; Haskell, B.A.; Fini, P.T.; Speck, J.S.; Nakamura, S. Ammonothermal growth of GaN utilizing negative temperature dependence of solubility in basic ammonia. *Mater. Res. Soc. Symp. Proc.* **2005**, *831*, E2.8. [CrossRef]
16. Hashimoto, T.; Fujito, K.; Saito, M.; Speck, J.S.; Nakamura, S. Ammonothermal growth of GaN on an over-1-inch seed crystal. *Jpn. J. Appl. Phys.* **2005**, *44*, L1570. [CrossRef]
17. Hashimoto, T.; Wu, F.; Speck, J.S.; Nakamura, S. Growth of bulk GaN crystals by the basic ammonothermal method. *Jpn. J. Appl. Phys.* **2007**, *46*, L889. [CrossRef]
18. Hashimoto, T.; Wu, F.; Speck, J.S.; Nakamura, S. A GaN bulk crystal with improved structural quality grown by the ammonothermal method. *Nat. Mater.* **2007**, *6*, 568–571. [CrossRef]
19. Dwilinski, R.; Doradzinski, R.; Garczynski, J.; Sierzputowski, L.P.; Puchalski, A.; Kanbara, Y.; Yagi, K.; Minakuchi, H.; Hayashi, H. Excellent crystallinity of truly bulk ammonothermal GaN. *J. Cryst. Growth* **2008**, *310*, 3911–3916. [CrossRef]
20. Wang, B.; Bliss, D.; Suscavage, M.; Swider, S.; Lancto, R.; Lynch, C.; Weyburne, D.; Li, T.; Ponce, F.A. Ammonothermal growth of high-quality GaN crystals on HVPE template seeds. *J. Cryst. Growth* **2011**, *318*, 1030–1033. [CrossRef]
21. Bao, Q.; Saito, M.; Hazu, K.; Kagamitani, Y.; Kurimoto, K.; Tomida, D.; Qiao, K.; Ishiguro, T.; Yokoyama, C.; Chichibu, S.F. Ammonothermal growth of GaN on a self-nucleated GaN seed crystal. *J. Cryst. Growth* **2014**, *404*, 168–171. [CrossRef]
22. Pimputkar, S.; Kawabata, S.; Speck, J.S.; Nakamura, S. Improved growth rates and purity of basic ammonothermal GaN. *J. Cryst. Growth* **2014**, *403*, 7–17. [CrossRef]
23. Hashimoto, T.; Letts, E.R.; Key, D.; Jordan, B. Two inch GaN substrates fabricated by the near equilibrium ammonothermal (NEAT) method. *Jpn. J. Appl. Phys.* **2019**, *58*, SC1005. [CrossRef]
24. Key, D.; Letts, E.; Hashimoto, T. Near-colorless free-standing bulk GaN c-plane substrates with excellent crystal quality grown by the ammonothermal method. In Proceedings of the 13th International Conference on Nitride Semiconductors, Washington, DC, USA, 7–12 July 2019.
25. Letts, E.; Key, D.; Hashimoto, T. Reduction of crack density in ammonothermal bulk GaN growth. *J. Cryst. Growth* **2016**, *456*, 27–32. [CrossRef]
26. Hashimoto, T.; Letts, E.; Key, D.; Male, K.; Michaels, M.; Hoff, S. Ammonothermal Bulk GaN Growth and Its Processing. *Sens. Mater.* **2014**, *26*, 385–392.
27. Letts, E.; Sun, Y.; Key, D.; Jordan, B.; Hashimoto, T. X-ray characterization technique for the assessment of surface damage in GaN wafers. *J. Cryst. Growth* **2018**, *501*, 13–17. [CrossRef]
28. Iso, K.; Ikeda, H.; Gouda, R.; Mochizuki, T.; Izumisawa, S. Annihilation mechanism of V-shaped pits in c-GaN grown by hydride vapor-phase epitaxy. *Jpn. J. Appl. Phys.* **2019**, *58*, SC1011. [CrossRef]